Title

Perturbations of Phosphatidate Cytidylyltransferase (CdsA) Mediate Daptomycin Resistance in Streptococcus mitis/oralis by a Novel Mechanism

Journal

Antimicrobial Agents and Chemotherapy, 61(4)

ISSN

0066-4804

Authors

Mishra, Nagendra N
Tran, Truc T
Seepersaud, Ravin
et al.

Publication Date

2017-04-01

DOI

10.1128/aac.02435-16

Peer reviewed

AMERICAN SOCIETY FOR MICROBIOLOGY | Antimicrobial Agents and Chemotherapy®

MECHANISMS OF RESISTANCE

Perturbations of Phosphatidate Cytidylyltransferase (CdsA) Mediate Daptomycin Resistance in *Streptococcus mitis/oralis* by a Novel Mechanism

Nagendra N. Mishra,[a,b] Truc T. Tran,[c] Ravin Seepersaud,[d,e] Cristina Garcia-de-la-Maria,[f] Kym Faull,[b] Alex Yoon,[b] Richard Proctor,[g] Jose M. Miro,[f] Michael J. Rybak,[h] Arnold S. Bayer,[a,b] Cesar A. Arias,[c,i] Paul M. Sullam[d,e]

LA Biomedical Research Institute, Torrance, California, USA[a]; Geffen School of Medicine at UCLA, Los Angeles, California, USA[b]; Center for Antimicrobial Resistance and Microbial Genomics, Division of Infectious Diseases, University of Texas McGovern School of Medicine, Houston, Texas, USA[c]; University of California, San Francisco, California, USA[d]; VA Medical Center, San Francisco, California, USA[e]; Hospital Clinic, Institut d'Investigacions Biomèdiques August Pi i Sunyer, University of Barcelona, Barcelona, Spain[f]; Departments of Medical Microbiology & Immunology and Medicine, University of Wisconsin School of Medicine and Public Health, Madison, Wisconsin, USA[g]; Anti-Infective Research Laboratory, Eugene Applebaum College of Pharmacy and Health Sciences, Wayne State University, Detroit, Michigan, USA[h]; Antimicrobial Resistance Unit and International Center for Microbial Genomics, Universidad El Bosque, Bogota, Colombia[i]

ABSTRACT *Streptococcus mitis/oralis* is an important pathogen, causing life-threatening infections such as endocarditis and severe sepsis in immunocompromised patients. The β-lactam antibiotics are the usual therapy of choice for this organism, but their effectiveness is threatened by the frequent emergence of resistance. The lipopeptide daptomycin (DAP) has been suggested for therapy against such resistant *S. mitis/oralis* strains due to its *in vitro* bactericidal activity and demonstrated efficacy against other Gram-positive pathogens. Unlike other bacteria, however, *S. mitis/oralis* has the unique ability to rapidly develop stable, high-level resistance to DAP upon exposure to the drug both *in vivo* and *in vitro*. Using isogenic DAP-susceptible and DAP-resistant *S. mitis/oralis* strain pairs, we describe a mechanism of resistance to both DAP and cationic antimicrobial peptides that involves loss-of-function mutations in *cdsA* (encoding a phosphatidate cytidylyltransferase). CdsA catalyzes the synthesis of cytidine diphosphate-diacylglycerol, an essential phospholipid intermediate for the production of membrane phosphatidylglycerol and cardiolipin. DAP-resistant *S. mitis/oralis* strains demonstrated a total disappearance of phosphatidylglycerol, cardiolipin, and anionic phospholipid microdomains from membranes. In addition, these strains exhibited cross-resistance to cationic antimicrobial peptides from human neutrophils (i.e., hNP-1). Interestingly, CdsA-mediated changes in phospholipid metabolism were associated with DAP hyperaccumulation in a small subset of the bacterial population, without any binding by the remaining larger population. Our results indicate that CdsA is the major mediator of high-level DAP resistance in *S. mitis/oralis* and suggest a novel mechanism of bacterial survival against attack by antimicrobial peptides of both innate and exogenous origins.

KEYWORDS *Streptococcus mitis/oralis*, daptomycin resistance, phosphatidate cytidylyltransferase

Received 22 November 2016 **Returned for modification** 21 December 2016 **Accepted** 1 January 2017

Accepted manuscript posted online 23 January 2017

Citation Mishra NN, Tran TT, Seepersaud R, Garcia-de-la-Maria C, Faull K, Yoon A, Proctor R, Miro JM, Rybak MJ, Bayer AS, Arias CA, Sullam PM. 2017. Perturbations of phosphatidate cytidylyltransferase (CdsA) mediate daptomycin resistance in *Streptococcus mitis/oralis* by a novel mechanism. Antimicrob Agents Chemother 61:e02435-16. https://doi.org/10.1128/AAC.02435-16.

Address correspondence to Arnold S. Bayer, abayer@labiomed.org, or Cesar A. Arias, cesar.arias@uth.tmc.edu.

N.N.M., T.T.T., and R.S. contributed equally to this work. A.S.B. and P.M.S. contributed equally to this work.

Overall, among the viridans group streptococci, *Streptococcus mitis/oralis* is one of the most important causes of serious community- and hospital-acquired infections, especially infective endocarditis (IE). In addition, this pathogen is particularly relevant in neutropenic cancer patients, causing life-threatening bacteremias (1, 2). A

major problem associated with *S. mitis/oralis* infections is the emergence of antimicrobial resistance. Indeed, *S. mitis/oralis* strains are frequently resistant *in vitro* to penicillin (~20 to 40% of isolates) and cephalosporin antibiotics, including third-generation agents such as ceftriaxone (~10 to 25% of isolates) (3–5), with occasional reports of treatment failure (6). Moreover, the use of vancomycin in *S. mitis/oralis* infections is limited by antibiotic tolerance to this agent (7). The restricted *in vitro* efficacy of β-lactams and vancomycin has led to the consideration of other therapeutic options for deep-seated *S. mitis/oralis* infections, such as newer cephalosporins (ceftaroline and ceftobiprole) and glyco- and lipopeptides such as telavancin and daptomycin (DAP). DAP, a lipopeptide antibiotic with potent *in vitro* activity against Gram-positive organisms, including *S. mitis/oralis*, has been used in severe infections caused by isolates exhibiting β-lactam resistance. However, *S. mitis/oralis* strains seem to be less susceptible to DAP than are other streptococci, with MICs that are 2- to 10-fold higher than those for other viridans group streptococci. In addition, *S. mitis/oralis* isolates have the unique propensity to develop rapid and sustained high-level resistance to DAP *in vivo* and *in vitro*, with MICs that are well above those observed for other DAP-resistant (DAP^r) Gram-positive organisms of clinical importance (8, 9).

Recent data suggest that the bactericidal activity of DAP depends on several important interactions of the antibiotic with the cell membrane, interfering with both fluid membrane microdomains and the preferential localization of the drug at the division septum (10–12). DAP seems to target fluid phospholipids in the outer leaflet of the cell membrane by a process that requires Ca^{2+} and possibly phosphatidylglycerol (PG), a major phospholipid constituent of bacterial membranes (12–14). PG and Ca^{2+} trigger the oligomerization of DAP in the outer leaflet of the membrane, after which the DAP oligomer reaches the inner leaflet in a process that appears to be influenced by the amount of cardiolipin (CL) (14, 15). Recent events have challenged the notion that the principal mechanism of DAP action is the formation of pores in the cell membrane; instead, it is thought that DAP binding and oligomerization result in the mislocalization of important proteins (such as MurG and PlsX, involved in lipid II synthesis and phospholipid metabolism) that disrupt cell wall and membrane homeostasis, leading to cell death (12). Of note, the mechanism of DAP action resembles those of many host defense cationic antimicrobial peptides (CAMPs), which also target the cell membrane (13).

Coresistance to DAP and CAMPs in Gram-positive cocci appears to be mediated by two major mechanisms: (i) repulsion of the antimicrobial peptide from the cell surface, thereby hindering the interaction of the antibiotic with the membrane target (13) (*Staphylococcus aureus* and *Enterococcus faecium*), and (ii) diversion of the antibiotic molecule away from the division septum (the principal target of DAP), in a process that is associated with an important remodeling of cell membrane phospholipids. In particular, the relocalization of anionic phospholipid microdomains away from the septum in *Enterococcus faecalis* is a prominent feature of the latter diversion mechanism (16). Here, we describe a distinct and unique mechanism of coresistance to DAP and CAMPs (seen both *in vivo* and *in vitro*) in the pathogen *S. mitis/oralis*. This novel strategy involves mutations in *cdsA*, encoding a phosphatidate cytidylyl transferase that catalyzes the synthesis of the phospholipid intermediate cytidine diphosphate (CDP)-diacylglycerol, a precursor for the production of PG and CL. Genetic changes result in an unusual phenotype that involves the complete loss of PG and CL from the cell membrane and the selective hyperaccumulation of DAP essentially within a small subpopulation of bacteria.

RESULTS

Generation of DAP^r *S. mitis/oralis* strain 351. DAP^r strains used in this study were derived both *in vitro* and *in vivo* (Table 1). For *in vitro* derivations, we exposed a DAP-susceptible (MIC = 0.5 μg/ml) human clinical bloodstream isolate, *S. mitis/oralis* 351, to increasing concentrations of DAP *in vitro*. After 10 days of serial DAP exposures at 20 μg/ml, we were able to select a high-level and stable DAP^r strain (*S. mitis/oralis*

TABLE 1 Bacterial strains and plasmids[a]

Strain or plasmid	Relevant characteristic(s)	DAP MIC (μg/ml)	Reference or source
Strains			
S. mitis/oralis			
351	Endocarditis isolate from a patient	0.5	8
351-D6-6	DAP^r derivative obtained *in vivo* in a rabbit endocarditis model	>256	8
351-D10	DAP^r derivative produced by *in vitro* passage	>256	This study
PS3473	*S. mitis/oralis* 351 Δ*cdsA*::*cat*	>256	This study
PS3487	*S. mitis/oralis cdsA*-3′ UTR::*cat*	0.5	This study
PS3488	*S. mitis/oralis* 351-D10 3′ *cdsA*::*cat*	0.5	This study
PS3489	*S. mitis/oralis* 351-D10 $cdsA_{D222N}$-3′ UTR::*cat*	>256	This study
PS3490	*S. mitis/oralis* 351 $cdsA_{D222N}$-3′ UTR::*cat*	>256	This study
E. coli TOP10	Host for cloning		Invitrogen
Plasmids			
pC326	*E. coli* vector with MCS::*cat*		29
pCdsA-KO	pC326 with *cat* flanked by 3′ *uppS* and 5′ *rseP* (segments from the genomic regions upstream and downstream of *cdsA*)		This study
pCdsA*cat*	pC326 with *cat* flanked by the 3′ half of *cdsA* and 5′ *rseP*		This study
$pCdsA_{D222N}$cat	pC326 with *cat* flanked by the 3′ half of $cdsA_{D222N}$ and 5′ *rseP*		This study

[a]DAP, daptomycin; MCS, multiple-cloning site; UTR, untranslated region. *uppS* and *rseP* are the ORFs immediately upstream and downstream of *cdsA*, respectively.

351-D10). Of note, high-level DAP^r (MIC > 256 μg/ml) (note that we use the term "daptomycin resistance" rather than "daptomycin nonsusceptibility" in this paper for ease of presentation) was stably maintained in this strain after 5 days of growth in the absence of DAP. For the *in vivo* derivation of DAP^r, we employed the rabbit IE model (8), using *S. mitis/oralis* strain 351 as the infecting strain. High-level DAP^r (MICs > 256 μg/ml) emerged in the cardiac vegetations of infected animals after only 48 h of treatment with DAP at a human-equivalent dose mimicking 6 mg/kg of body weight (strain 351-D6-6), as previously reported (8).

Genetic basis of DAP^r in *S. mitis/oralis*. To identify the genetic basis for DAP^r, we performed whole-genome sequencing of *S. mitis/oralis* strains 351, 351-D10, and 351-D6-6 (see Table 1 and also Table S2 in the supplemental material, respectively) (8). In 351-D10, comparative analyses identified seven predicted open reading frames (ORFs) containing single nucleotide polymorphisms (SNPs) (Table 2). Among the genes identified, ORF *sm351-26* was of high interest, since it encodes a predicted phosphatidate cytidylyltransferase (CdsA). This enzyme is a transmembrane protein responsible for the synthesis of CDP-diacylglycerol, using CTP and phosphatidic acid (PA) as the substrates. CDP-diacylglycerol is the substrate for PgsA, the enzyme responsible for PG synthesis. Subsequently, two molecules of PG are utilized for the synthesis of CL by cardiolipin synthase (Fig. 1A). Like other CdsA homologues, CdsA of *S. mitis/oralis* is predicted to be a membrane protein with nine transmembrane domains (Fig. 1B). Modeling of *S. mitis/oralis* CdsA on the structure of CdsA of *Thermotoga maritima* (TmCdsA) (17) suggests a similar topological organization, with cytosolic binding loops (A loop and B loop) and the conserved SPXKXXEG and HGGXXDRXD motifs necessary for binding CTP and phosphatidate (Fig. 1B and Fig. S1). Interestingly, the substitution

TABLE 2 Genetic changes associated with daptomycin resistance in *S. mitis/oralis* 351-D10

ORF	Gene	Predicted amino acid substitution	Predicted function
sm351-26	*cdsA*	D222N	Phosphatidate cytidylyltransferase
sm351-42	*rpoB*	F988L	DNA-directed RNA polymerase, b subunit
sm351-129	*fni*	L280V	Isopentyl-diphosphate delta isomerase
sm351-251		R169stop	Uncharacterized membrane protein
sm351-669	*pepT*	V40I	N-terminal amino acid peptidase of tripeptides
sm351-1076	*rbn*	P53H	RNase BN
sm351-1167	*clpX*	C251F	ATP-dependent Clp protease ATP-binding subunit ClpX

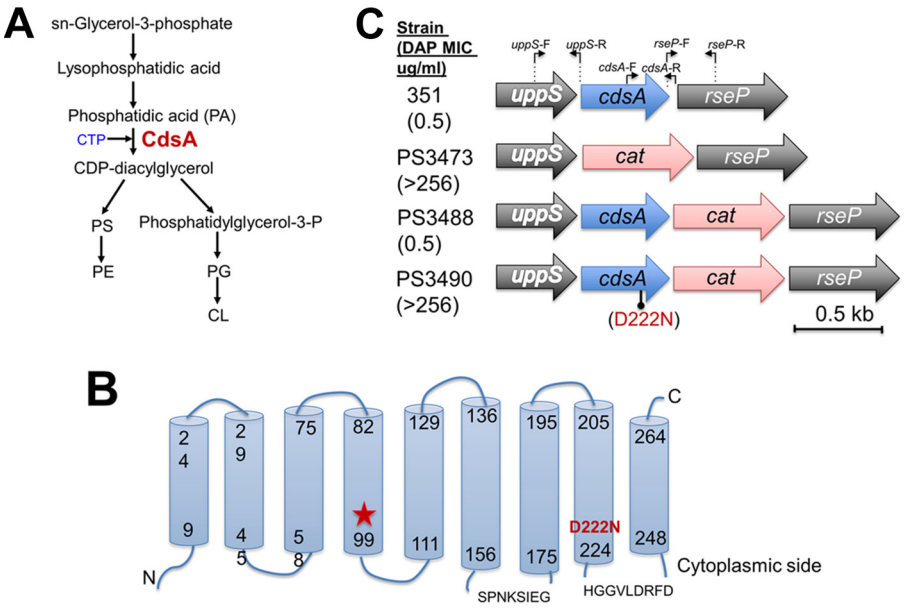

FIG 1 Changes in CdsA cause daptomycin resistance in *S. mitis/oralis*. (A) Schematic representation of the synthesis of major cell membrane phospholipids in bacteria. CdsA uses CTP and phosphatidic acid to produce CDP-diacylglycerol, a precursor of the synthesis of phosphatidylglycerol (PG), cardiolipin (CL), phosphatidylserine (PS), and phosphatidylethanolamine (PE). (B) CdsA of *S. mitis/oralis* 351 is predicted to have nine transmembrane domains. The conserved CTP and phosphatidate substrate-binding loops SPXKXXEG and HGGXXDRXD are shown, as is the location of the D222N substitution found in 351-D10 and the frameshift mutation (red star). (C) *cdsA* locus in *S. mitis/oralis* 351 and derivatives. The locations of oligonucleotide annealing sites for PCR primers are shown above the loci.

found in 351-D10 CdsA was an Asp222→Asn substitution located in the eighth predicted transmembrane helix. Asp222 of *S. mitis/oralis* CdsA aligned with Asp219 of TmCdsA, which forms part of a cation-binding Asp-Asp dyad essential for enzymatic activity (17) (Fig. S1). Similarly, the *in vivo*-derived DAP^r *S. mitis/oralis* variant strain 351-D6-6 was found to have a 2-bp deletion after codon 91 in *cdsA*, leading to a frameshift that disrupts the predicted enzyme (Fig. 1B). Collectively, our findings strongly indicate that the mutations in *cdsA* found in DAP^r *S. mitis/oralis* strains 351-D10 and 351-D6-6 would result in markedly reduced or abolished enzymatic activity.

To confirm the role of the *cdsA* mutations in DAP resistance, we generated a series of gene replacements using a chloramphenicol resistance gene (*cat*) cassette. Our initial approach employed allelic exchange to replace the entire *cdsA* gene with a *cat* cassette. Although *cdsA* was previously described as an essential gene in *Escherichia coli* (18, 19), we were successful in generating a *cdsA*-null mutant in *S. mitis/oralis* 351 (strain PS3473) (Fig. 1C and Table 1). The deletion of *cdsA* caused a marked growth defect in the strain, exhibiting a delay in the logarithmic phase in Todd-Hewitt broth (THB) (see Fig. S2 in the supplemental material). Moreover, colonies of PS3473 were smaller than those of *S. mitis/oralis* 351 and had a pitted appearance. Despite this growth defect, PS3473 exhibited stable high-level DAP resistance (MIC $>$ 256 μg/ml), confirming that the loss of *cdsA* is responsible for the DAP^r phenotype. We then attempted to complement the above-described mutation in *trans* with wild-type *cdsA*, which proved unsuccessful (data not shown). We therefore opted for an allelic replacement strategy in which *cdsA* harboring a D-to-N mutation at position 222 ($cdsA_{D222N}$) in *S. mitis/oralis* 351-D10 was replaced by the wild-type *cdsA* allele from 351 (generating strain PS3488) and wild-type *cdsA* in *S. mitis/oralis* 351 was replaced with the $cdsA_{D222N}$ allele (generating strain PS3490) (Fig. 1C and Table 1). These allelic exchanges resulted in an increased DAP susceptibility (DAP^s) of PS3488 to wild-type levels (MIC of 0.5 μg/ml) and DAP resistance in PS33490 (MIC $>$ 256 μg/ml). These data confirmed that mutagenesis of *cdsA* was sufficient to confer high-level DAP resistance.

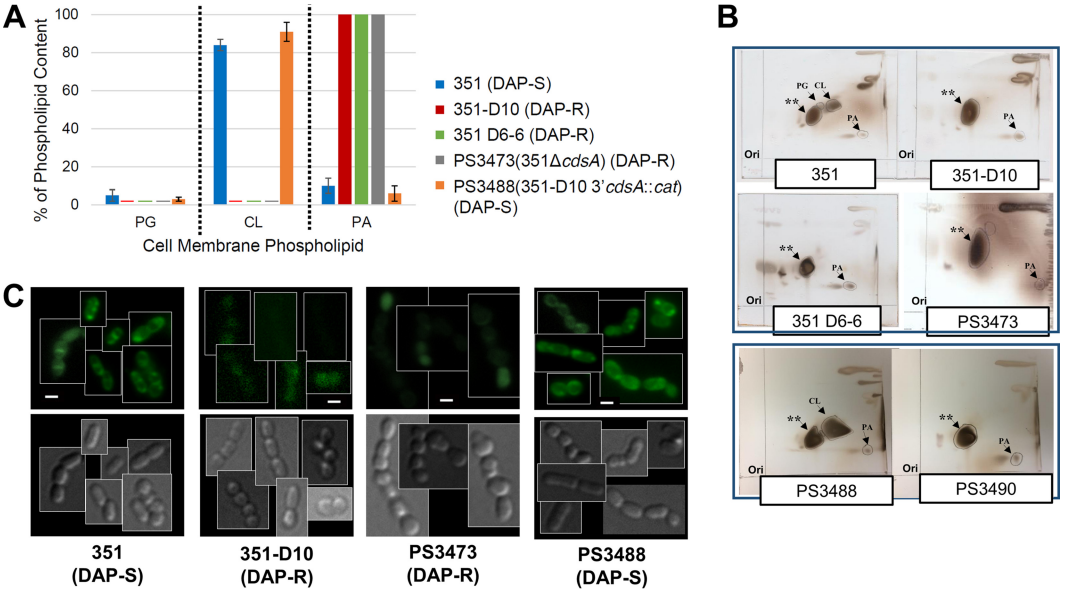

FIG 2 Major cell membrane phospholipids of *S. mitis/oralis* strains. Proportions of PG, CL, and PA in cell membranes of *S. mitis/oralis* and derivatives were determined by 2D thin-layer chromatography. (A) Development of daptomycin resistance is associated with the disappearance of PG and CL. The deletion of *cdsA* resulting in daptomycin resistance also recapitulates the same phospholipid profile (PS3473). The reintroduction of the wild-type *cdsA* allele into 351-D10 (strain PS3488) reverses this phenotype. (B) 2D thin-layer chromatography of *S. mitis/oralis* derivatives. Spots corresponding to PG and CL disappear in *S. mitis/oralis* 351-D10 and 351-D6-6. Knockout of *cdsA* in 351 results in the same phenotype (PS3473). The introduction of a wild-type *cdsA* allele in 351-D10 reverts the phenotype (strain PS3488). The introduction of a mutated *cdsA* allele into 351 recapitulates the DAP^r phenotype and phospholipid abnormalities (strain PS3490). **, copurified glycolipid found in all *S. mitis/oralis* strains and identified as digalactosyldiacylglycerol by mass spectrometry. (C) NAO staining of *S. mitis/oralis* to detect anionic phospholipid microdomains. The development of daptomycin resistance is associated with no discernible visualization of phospholipid microdomains. The deletion of *cdsA* also yields the same phenotype. The reintroduction of the wild-type *cdsA* allele into daptomycin-resistant strain 351-D10 (strain PS3488) restores the visualization of anionic phospholipid microdomains.

Mutations in *cdsA* result in major changes in cell membrane phospholipid content and order. As noted above, the cell membrane phospholipid content plays a major role in the mechanism of DAP action. We therefore compared the phospholipid content of the DAP^s parental *S. mitis/oralis* strain 351 with its DAP^r derivatives 351-D10 and 351-D6-6. The development of DAP^r was associated with a striking reduction in the levels of both PG and CL in both mutants, to amounts that were below the level of detection in two-dimensional (2D) thin-layer chromatography (TLC) assays. The lack of PG and CL was associated with a proportional increase in the level of PA, the substrate for CdsA activity (Fig. 2A and B), which was confirmed by electrospray ionization mass spectrometry (data not shown).

We subsequently stained the cells with 10-*N*-nonyl acridine orange (NAO) to localize cell membrane anionic phospholipid microdomains, which are thought to be formed mainly with CL, although PG (the DAP target phospholipid) was also recently identified (20). Of note, phospholipid microdomains play an important role in the diversion mechanism of DAP^r in *E. faecalis* (16). We were able to readily identify anionic phospholipid microdomains in the membranes of *S. mitis/oralis* 351 cells (Fig. 2C). In contrast, we did not detect any microdomains in the cell membranes of the DAP^r derivatives of *S. mitis/oralis* 351D-10 (Fig. 2C). Similarly, the deletion of *cdsA* (strain PS3473) also resulted in a lack of visible anionic phospholipid microdomains. In turn, replacement of the mutated *cdsA* allele with a wild-type copy in 351-D10 (strain PS3488) restored the visualization of such microdomains (Fig. 2C). These data strongly indicate that the loss of CdsA function abolishes the production of CL and PG, resulting in DAP^r.

We also investigated the relative state of cell membrane order (fluidity versus rigidity), since this property has been shown to have a profound impact on the ability of CAMPs (such as calcium-DAP and host defense peptides [HDPs]) to interact with

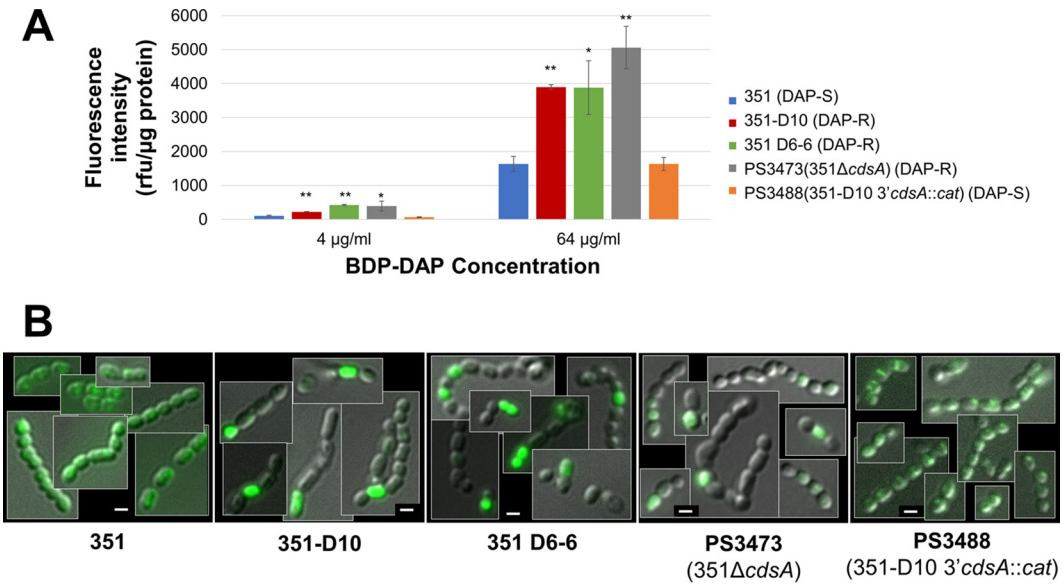

FIG 3 Mechanism of DAP resistance in *S. mitis/oralis* 351. (A) Fluorescence intensity normalized to the protein ratio using BDP-DAP binding to *S. mitis/oralis*. The development of DAP resistance is associated with a significant increase in drug binding in DAP^r strains 351-D6-6 and 351-D10. The increased binding can be replicated by the deletion of *cdsA* in wild-type strain 351 (strain PS3473). Restoration of the wild-type *cdsA* allele in 351-D10 (strain PS3488) reverses the phenotype. **, $P < 0.0001$; *, $P < 0.005$. rfu, relative fluorescence units. (B) BDP-DAP binding was evaluated by fluorescence microscopy. The images within each panel show bacterial cells captured by fluorescence and phase-contrast microscopy. Hyperaccumulation of BDP-DAP in a few cells is evident in DAP^r strains 351-D10 and 351-D6-6. The phenotype can be reproduced by the deletion of *cdsA* in 351. Restoration of the wild-type *cdsA* allele in 351-D10 (strain PS3488) reverses the phenotype.

target membranes. Previous studies have shown that for cell membrane-targeting cationic peptides, there is an optimal degree of membrane order for maximal interaction (21, 22). In addition, most DAP^r *S. aureus* strains and some DAP^r enterococcal strains show signature alterations in cell membrane order (21, 23). By using polarization spectrofluorimetry to compare parental *S. mitis/oralis* strain 351 to DAP^r strain 351-D10, the development of DAP^r was associated with a significant increase in membrane fluidity (see Table S3 in the supplemental material).

CdsA-mediated DAP^r results in selective hyperconcentration of the antibiotic. We next sought to investigate whether the *cdsA*-mediated changes in *S. mitis/oralis* resulted from mechanisms of DAP^r found previously in other Gram-positive bacteria (repulsion versus diversion). Both DAP^r strains had significant increases in the overall binding of Bodipy FL-labeled DAP (BDP-DAP) compared with the parental strain (Fig. 3A), indicating that the mechanism of resistance did not involve DAP repulsion from the bacterial surface. We then investigated the distribution of BDP-DAP binding by high-resolution fluorescence microscopy. As expected, the parental DAP-susceptible *S. mitis/oralis* strain 351 had uniform BDP-DAP binding to most cells (Fig. 3B), as was described previously for other species (10, 16). In contrast, in the DAP^r derivatives 351-D6-6 and 351-D10, only a few selected cells within a given chain bound large amounts of BDP-DAP, with the majority of cells lacking evidence of any BDP-DAP binding (Fig. 3B). This pattern of antibiotic binding was also seen in the *cdsA* deletion variant PS3473. The introduction of the wild-type *cdsA* allele to 351-D10 reverted BDP-DAP binding by the resulting transformant PS3488 to the uniform-distribution phenotype seen with the wild-type strain (Fig. 3B). Thus, our findings indicate that in contrast to what has been reported for other species, DAP^r variants of *S. mitis/oralis* neither repel nor divert the antibiotic from the target sites. Instead, changes in CdsA result in a novel phenomenon that involves selective DAP hyperconcentration within a small subpopulation of cells, in conjunction with a loss of uptake by the larger population of bacteria.

Impact of DAP hyperaccumulation on DAP^r *S. mitis/oralis* upon cell viability. We subsequently assessed the effects of the above-mentioned selective DAP binding on

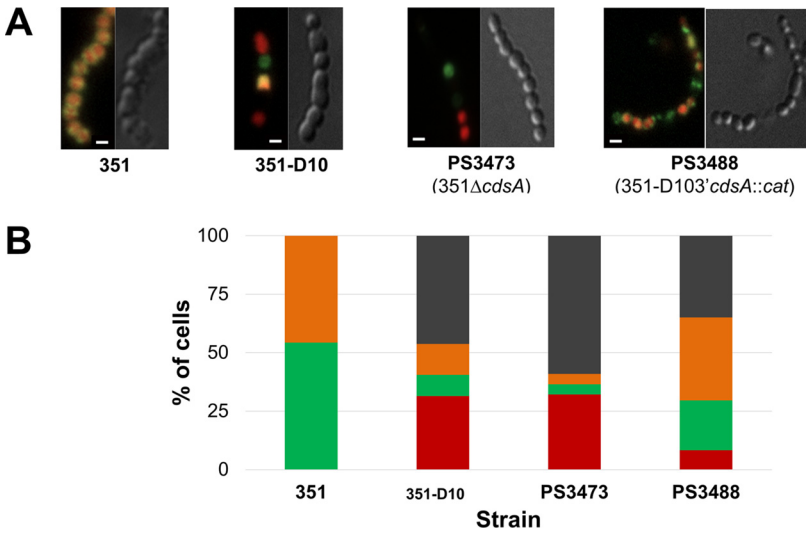

FIG 4 Viability (propidium iodide) and BDP-DAP staining of *S. mitis/oralis* cells. (A) BDP-DAP (green), propidium iodide (red), and overlay (orange) staining to assess for cell membrane permeabilization (as a surrogate of bacterial cell death). Unstained cells represent "survivors," in which the antibiotic does not bind and permeabilization by PI does not occur. The proportion of unstained cells is markedly increases in DAP^r strain 351-D10 and in *S. mitis/oralis* 351 carrying the *cdsA* deletion (strain P3473). Restoration of the wild-type *cdsA* allele in 351-D10 (strain PS3488) reverses the phenotype. Bar, 1 μm. (B) Proportion of cells stained with BDP-DAP (green), propidium iodide (red), both (orange), or none (black) in 100 cells chosen randomly in a field. The proportion of survivors was markedly increased from 0% for 351 to up to 50% for all daptomycin-resistant derivatives. However, a lack of membrane viability occurs in similar proportions in cells that take up the antibiotic versus those that do not hyperconcentrate BDP-DAP.

cell viability, using dual staining with BDP-DAP plus propidium iodide (PI) (Fig. 4). Since DAP alters cell membrane integrity, leading to the eventual death of bacteria, nonviable bacteria with disrupted membranes can be identified by their intracellular uptake of PI (24). We analyzed the proportion of cells that bound BDP-DAP alone, PI alone, both fluorophores, or neither dye for strains 351, 351-D10, and other isogenic variants. Parental strain 351 exhibited uniform binding (100% of cells) with BDP-DAP (green fluorescence), which was accompanied by a concomitant uptake of PI (orange fluorescence) by about 50% of the total population (Fig. 4A). This pattern of fluorescence in *S. mitis/oralis* 351 suggests that membrane damage is occurring in a significant proportion of the population upon DAP binding and that these cells are not viable. In contrast, 351-D10 showed a pattern with a mixed population of cells that bound either BDP-DAP or PI, with little overlap of the two populations (i.e., with only ~13% being dually labeled). Moreover, the proportion of cells with no staining with either fluorophore was markedly increased in 351-D10 (~ 50%) compared with that for 351 (0%) (Fig. 4B). The deletion of *cdsA* in 351 (PS3473) resulted in a phenotype that was almost identical to that of 351-D10, with ~60% of cells having no dye uptake and relatively few dually labeled bacteria. The replacement of *cdsA* in 351-D10 (PS3488) with the wild-type *cdsA* allele increased the proportion of dual staining to levels comparable to those seen with parental strain 351 (Fig. 4B). Collectively, these results indicate that the mutagenesis of *cdsA* results in a novel DAP^r phenotype, characterized by the selective binding of DAP in a small subpopulation of DAP^r cells, coupled with a larger population of viable survivor cells that do not bind DAP.

Cross-resistance between DAP and CAMPs. Our previous studies (21–23, 25) indicated that the development of DAP^r in *S. aureus* and enterococci was associated with concomitant cross-resistance to other cationic peptides, including several of human polymorphonuclear cell origin. This property would potentially give DAP^r isolates additional survival advantages once in the bloodstream, by providing resistance to the antibiotic as well as evasion of the innate immune system. Thus, we compared *S. mitis/oralis* 351 and 351-D10 for relative susceptibilities to two distinct, granule-stored

polymorphonuclear peptides, LL-37 and hNP-1. Interestingly, *S. mitis/oralis* 351-D10 exhibited a significant increase in survival against hNP-1 compared to 351 (~3.3-fold and 4.8-fold when exposed to 80 and 40 μg/ml DAP, respectively; $P < 0.05$) (see Table S4 in the supplemental material). A similar trend was noted for LL-37, although these differences did not reach statistical significance.

DISCUSSION

Our findings indicate that DAP^r in *S. mitis/oralis* is mediated by a mechanism that involves a loss of function of CdsA, a major enzyme in the synthesis of cell membrane phospholipids. To the best of our knowledge, CdsA has not been previously implicated in resistance to DAP or other CAMPs. CdsA encodes a critical enzyme for the synthesis of CDP-diacylglycerol, an essential precursor of both PG and CL. Using the crystal structure of CdsA from *T. maritima* (17) as a template, we determined that the substitution found in 351-D10 CdsA replaces Asp222, a residue that is predicted to be part of a dyad coordinating a Mg^{2+}-K^+ heterodimetal center that serves as a cofactor for the enzyme. The *cdsA* frameshift found in 351-D6-6 results in a truncated peptide that lacks the residues necessary to form the heterodimetal center, rendering the enzyme nonfunctional. Additionally, the frameshift does not appear to affect the downstream gene (*rseP*) (Fig. 1C) since it does not affect its ribosomal binding sites or the predicted start codon. Our results support these predictions, since we did not detect either PG or CL in the cell membranes of DAP^r derivatives of *S. mitis/oralis* 351. In addition, we were unable to identify anionic phospholipid microdomains in the cell membranes of resistant strains, which are thought to be formed mainly by CL (and perhaps PG) (20). Although it is possible that our assays were not sensitive enough to detect minute amounts of these phospholipids, the striking difference in membrane content compared with that of parental DAP^s *S. mitis/oralis* strain 351 strongly indicates that the *cdsA* mutations markedly decreased the predicted function of CdsA. The loss of function of CdsA results in a major effect on the phospholipid content of the cell membrane, with a disappearance of PG (and CL) in DAP^r strains, the main cell membrane target of DAP. A reduction of the PG content in cell membranes was previously associated with DAP^r in other Gram-positive organisms such as *Bacillus subtilis*, *S. aureus*, and enterococci (26–28). However, no single biosynthetic gene (i.e., *cdsA*) was previously shown to have such a large impact on membrane composition, underscoring the unprecedented and complete disappearance of two key downstream membrane phospholipids that we observed. We postulate that the absence of PG would preclude DAP oligomerization in the cell membrane, preventing subsequent antibiotic-mediated killing.

In the absence of PG and CL, it is likely that DAP^r *S. mitis/oralis* strains use other phospholipids to maintain a functional cell membrane, although such a replacement appears to compromise cell fitness. Thus, our results clearly indicate that changes in CdsA were sufficient to confer DAP^r at the expense of a decrease in fitness in terms of cell growth kinetics. In addition, these *cdsA* mutants are also modestly less fit in experimental IE (29). Overall, these data suggest that the observed *cdsA* mutation has a deleterious effect on cell physiology and is likely the result of antibiotic pressure. Since other changes were found in the genomes of the DAP^r derivatives (Table 1; see also Fig. S2 in the supplemental material), it is likely that the affected genes compensate for the major fitness cost brought about by mutations in *cdsA*. Interestingly, it has been shown that *E. coli* cells lacking PG can grow almost normally in rich medium if the major outer membrane lipoprotein is deficient (30), indicating that PG and CL are nonessential for either cell viability or basic metabolic activities. Moreover, vancomycin-susceptible *E. coli* strains that carry mutations in the synthesis of lipopolysaccharide revert to vancomycin resistance when loss-of-function mutations in *cdsA* occur, resulting in the accumulation of PA, although the mechanisms for this change in susceptibility are not clear (31). Since *cdsA* was mutated in two independently derived DAP^r isolates of *S. mitis/oralis* selected under different conditions in our study, we can

conclude that *cdsA* is also not an essential gene in this organism and thus could have a major role in the development of CAMP resistance in *S. mitis/oralis*.

Mutagenesis of *cdsA* also produced a novel and striking phenotype, featuring high levels of selective DAP binding to a small subpopulation of surviving DAP^r bacteria. The mechanism(s) by which the loss of CdsA activity results in this unique pattern of distribution of DAP is unknown, as is its impact on viability. As discussed above, the absence of PG would remove the natural target of DAP and would explain the lack of antibiotic binding to the majority of the population, resulting in cell survival. However, we observed a somewhat different phenomenon in DAP^r strains, where about 25% of cells avidly bound DAP. One plausible explanation for the observed pattern of DAP binding is that selective DAP-hyperaccumulating cells may have reverted their *cdsA* mutation to the wild type and reconstituted the production of PG. This would theoretically, in turn, enhance selective DAP binding and protect the rest of the population. In this scenario, one would expect that this selected population of DAP-hyperaccumulating cells would perish, in an example of altruistic "suicide" that has been shown to occur in several Gram-positive organisms, especially within biofilms (32, 33). However, data from our microscopy studies do not support such a mechanism. Indeed, the ~45% of cells that avidly bound DAP appeared to remain viable, as indicated by a lack of PI uptake. On the other hand, about 30% of cells that did not bind DAP were stained by PI, suggesting nonviability (Fig. 4B). Of note, there is clearly a large subpopulation of cells of the DAP^r strains (but not of DAP^s isolates) that accumulate neither DAP nor PI and represent "protected survivor cells." Overall, these intriguing data suggest that *S. mitis/oralis* cells within a given subpopulation are able to individually adjust their CdsA activity to accomplish one of two goals: (i) loss-of-function mutations, resulting in the prevention of DAP accumulation in the majority of the DAP^r populations, or (ii), potentially, gains in function to enhance cell-specific DAP hyperaccumulation in a minority of cells, in a novel form of altruism. The precise mechanism(s) linking the loss of CdsA activity with the selective binding of DAP remains to be defined and is the object of our ongoing research efforts. This will likely require single-cell genomics analyses.

From a clinical perspective, the increasing rates of resistance to β-lactams in streptococci and the ability of these organisms to develop tolerance to vancomycin suggest that DAP may be considered an alternative agent to treat deep-seated infections in the future. Our data provide compelling *in vivo* and *in vitro* evidence that the use of DAP monotherapy in these severe infections may be associated with the rapid development of resistance, possibly leading to therapeutic failures. Optimizing the use of DAP in these circumstances is the objective of our ongoing research efforts.

MATERIALS AND METHODS

Bacterial isolates and growth conditions. Plasmids, bacterial strains, and mutant constructs used in this study and their respective MICs are shown in Table 1. For the DAP *in vitro* passage study, parental strain 351 was cultured overnight in brain heart infusion (BHI) broth. An initial inoculum at an optical density at 600 nm (OD_{600}) of 1 (~10^8 CFU/ml) was exposed to 20 μg/ml of DAP in BHI broth (plus 50 μg/ml $CaCl_2$). Surviving colonies after each 24-h exposure to DAP were then collected and passaged for 10 consecutive days; after passage each day, surviving colonies were stored at −80°C. The MICs of the parental strain and each of the DAP-passaged strains were determined by a standard Etest. To investigate the stability of any DAP^r isolates that appeared during the 10-day passage period, the postpassage DAP^r strains were again grown and passaged daily in antibiotic-free BHI broth for 5 days. The DAP MICs of these antibiotic-free postpassage isolates were retested by an Etest. *In vivo*-passaged DAP^r *S. mitis/oralis* strain 351-D6-6 was selected by using a rabbit endocarditis model as described previously (8). This strain was isolated from the cardiac vegetations of animals receiving 6 mg/kg of DAP once daily after 48 h of therapy (8).

For all genetic manipulations, *S. mitis/oralis* strains were grown in THB (Becton, Dickinson and Co.) or on sheep blood agar (Hardy Diagnostics) at 37°C in a 5% CO_2 environment. When indicated, antibiotics were added to the growth medium at the following concentrations: erythromycin at 50 μg/ml, chloramphenicol at 5 μg/ml, and DAP at 32 μg/ml. *E. coli* strain TOP10 was grown in Luria-Bertani (LB) broth or on LB agar containing chloramphenicol (15 μg/ml) or erythromycin (15 μg/ml) when appropriate. Determination of DAP MICs was carried out by a standard Etest on cation-adjusted Mueller-Hinton agar according to the manufacturer's recommendations after incubation at 37°C for 24 h, as described previously (16).

Bodipy-DAP uptake and cell viability staining with PI. BDP-DAP (Merck Co, Lexington, MA) is a fluorescent derivative of DAP that retains antimicrobial activity. We used BDP-DAP (at 4 and 64 μg/ml) to assess the interaction of DAP with our *S. mitis/oralis* strain set, as described previously (16, 25, 34). In assays with PI (24), staining with BDP-DAP was first performed by using a BDP-DAP concentration of 64 μg/ml. After the removal of excess unbound BDP-DAP, cells were washed twice in LB broth. PI (30 μM) was then added, and cells were then incubated at 37°C for 15 min. Cells were washed once with morpholinepropanesulfonic acid (MOPS) buffer (pH 7.2) and then immobilized on a coverslip pretreated with poly-L-lysine (Sigma-Aldrich). Bacterial cells were viewed with an Olympus IX71 fluorescence microscope equipped with PlanApo N 100× objective. Fluorescence was observed by using standard fluorescein isothiocyanate (FITC) (excitation at 490 nm and emission at 528 nm for BDP-DAP) and tetramethylrhodamine isothiocyanate (TRITC) (excitation at 541 nm and emission at 617 nm for PI) filter sets. Data acquisition was performed by using SlideBook 5.0 software. Protein extraction from each cell preparation was performed according to previously described methods in order to standardize our quantitative fluorescence analyses (16, 34). Protein concentrations were estimated by using the bicinchoninic acid (BCA) protein assay kit (Thermo Scientific) according to the manufacturer's instructions. A minimum of two independent experiments was performed for each strain on different days. Statistical analyses of fluorescence intensity were done by performing Student's unpaired *t* test, comparing DAP^r to DAP^s parental strains.

NAO staining. Visualization of cell membrane anionic phospholipid-rich microdomains was performed by using the fluorescent dye NAO as described previously (16, 35). Fluorescence imaging and phase-contrast imaging were performed on an Olympus IX71 microscope with a PlanApo N 100× objective. At least three independent sets of experiments were done for each strain on different days.

Cell membrane phospholipid content and fluidity. Lipid extractions from *S. mitis/oralis* strains were carried out as described previously (21, 22, 36). Briefly, *S. mitis/oralis* strains were grown in BHI broth for 18 h (to late stationary phase). The major *S. mitis/oralis* phospholipids were separated by 2D TLC (Silica 60 F254 HPTLC plates; Merck) (26). Individual phospholipids segregated from 2D TLC plates were demonstrated by digestion at 180°C for 3 h with 0.3 ml 70% perchloric acid and quantified spectrophotometrically at an OD_{660}, as reported previously (26). The data included results from a minimum of three independent experiments performed on separate days. The identification and confirmation of all spots on the TLC plate were carried out by exposure to iodine vapors, spraying with $CuSO_4$ (100 mg/ml) containing 8% (vol/vol) phosphoric acid, and heating at 180°C (37). We employed mass spectrometry to confirm the TLC spot identifications of all phospholipid species (see below). Fluidity assays were carried out as described previously (26), using the fluorescent probe 1,6-diphenyl-1,3,5-hexatriene (DPH). The protocol for DPH incorporation into target cell membranes, measurement of fluorescence polarization, and calculation of the fluorescence polarization index were described previously (38). There is an inverse relationship between polarization index values and membrane fluidity (22, 38). The mean (± standard deviation [SD]) polarization index values were obtained from a minimum of 3 to 5 independent experiments on separate days. Unpaired Student's *t* test was employed to compare constructs. A *P* value of <0.05 was considered statistically significant.

Electrospray ionization mass spectrometry. The lipid extracts described above were redissolved in chloroform–methanol–300 mM aqueous ammonium acetate (AA) (250 μl; 300/665/35, vol/vol/vol), injected onto a silica-based reversed-phase high-performance liquid chromatography (HPLC) column (Kinetex XB-C_{18}, 1.7 μm, 100 by 2.1 mm; Phenomenex) equilibrated in solvent A (methanol-chloroform [90/10, vol/vol] containing 5 mM AA), and eluted with increasing concentrations of solvent B (chloroform-water [500/0.2, vol/vol] containing 5 mM AA with 0 min of 0% solvent B/200 ml/min, 3 min of 0% solvent B/200 ml/min, 3 min of 0.1% solvent B/100 ml/min, 20.5 min of 100% solvent B/100 ml/min, 23 min of 100% solvent B/100 ml/min, 24 min of 0% solvent B/200 ml/min, and 30 min of 0% solvent B/200 ml/min). The effluent from the column was directed to an electrospray ion source (Agilent Jet Stream) (gas temperature of 300°C, gas flow of 6 liters/min, nebulizer pressure of 45 lb/in^2, sheath gas temperature of 50°C, sheath gas flow rate of 10 liters/min, capillary voltage of 4,500 V, and nozzle voltage of 2,000 V) connected to a triple-quadrupole mass spectrometer (Agilent 6460) for the collection of mass spectra, fragment ion mass spectra of preselected parents, and neutral-loss spectra. When operating in the negative-ion mode, 0.1% (vol/vol) triethylamine was substituted for AA in solvents A and B, and a polymeric reverse-phase column (PLRP-S; Agilent) (300Å, 5 μm, and 150 by 2 mm) was used. For each mode of operation, data were collected by using previously optimized conditions (instrumental parameters of fragmentor, collision energy, and collision accelerator voltage) determined by using authentic standards introduced by flow injection (50 μl/min) in a mixture of solvents A and B (50/50, vol/vol). Data were collected with software supplied by the instrument manufacturer (Agilent Mass Hunter version B.05.00).

CAMP assays of hNP-1 and LL-37 susceptibilities. To examine for potential DAP-CAMP coresistance, we employed two prototypic CAMPs that are contained in distinct human neutrophil granules, hNP-1 and LL-37. A bactericidal susceptibility assay was performed with 20% BHI broth plus 10 mM potassium phosphate buffer (PPB) by a 2-h time-kill method, as reported previously (23). Stationary-phase bacterial cells in a final inoculum $\sim 10^5$ CFU/ml were utilized. The hNP-1 and LL-37 concentrations used in this assay were 40 and 80 μg/ml and 5 and 10 μg/ml, respectively. These peptide concentrations were selected after extensive screening based on (i) sublethality, with $<50\%$ reductions in counts of the 351 parental (DAP^s) strain, and (ii) encompassing peptide concentrations utilized in previous investigations of hNP-1 and LL-37 interactions with *S. aureus* (23). The data are represented as mean (±SD) percentages of surviving CFU per milliliter compared to non-CAMP-exposed cells. There are no established "breakpoints" for the HDPs, so data were statistically compared by unpaired Student's *t* test, with

a *P* value of <0.05 being considered significant. A minimum of three independent runs were performed on different days.

DNA extraction and whole-genome sequencing. Genomic DNA from all strains was isolated by using a modified cetyltrimethylammonium bromide (CTAB) extraction method. A total of 50 ml of cultures was grown overnight in THB at 37°C. Bacteria were collected by centrifugation and resuspended in Tris-EDTA (TE) containing 100 U of mutanolysin and incubated at 37°C for 2 h. Cells were lysed in 0.5% sarcosyl followed by sequential treatment with RNase (30 U) and proteinase K (400 μg) and CTAB-NaCl extraction. DNA was precipitated in isopropanol and washed with 70% (vol/vol) ethanol. The precipitated DNA was further purified by using a PureLink Genome DNA minikit (Invitrogen) according to the manufacturer's instructions. PacBio library construction, sequencing, and annotation were performed by using standard methods (39, 40). Genome assemblies were generated by using Celera Assembler v8.2. (http://wgs-assembler.sourceforge.net/) and HGAP3 (PacBio). Gene annotation was performed by using the IGS microbial annotation pipeline (39). SNPs and short indels were identified by using the assembled contigs through an IGS-developed NUCmer-based pipeline called Skirret. The resulting SNPs were annotated by using SnpEff (40). All mutations identified by whole-genome sequencing were confirmed by PCR and Sanger sequencing.

Mutant construction and genetic manipulations. To generate a *cdsA* deletion mutant of strain 351, a gene replacement cassette was constructed by cloning the chromosomal regions flanking *cdsA* upstream and downstream of the chloramphenicol (*cat*) gene in pC326 (41). The resulting plasmid, pCdsA-KO, was introduced into *S. mitis/oralis* 351 by natural transformation, as previously described (42). For the construction of *cdsA* gene replacement strains, we replaced the $cdsA_{D222N}$ gene of strain 351-D10 with the wild-type ("susceptible") allele from 351. A *cdsA-cat* transcriptional fusion cassette was first constructed by amplifying a 684-bp fragment encompassing the 3′ half of *cdsA* together with 7 bp of the adjacent intergenic region with primer pair cdsA-F and cdsA-R (see Table S1 in the supplemental material), using *S. mitis/oralis* 351 genomic DNA as the template (Fig. 1C). The amplified DNA was digested with XhoI and ClaI and cloned upstream of the *cat* gene in pC326. A 504-bp downstream fragment was generated as described above for constructing pCdsA-KO and cloned downstream of the *cat* cassette. The resulting plasmid, pCdsA*cat*, was introduced into *S. mitis/oralis* 351-D10 by natural transformation, followed by plating onto blood agar containing chloramphenicol. PCR amplification and DNA sequencing of the resulting colonies confirmed that the $cdsA_{D222N}$ gene had been replaced by *cdsA*, with *cat* being inserted into the adjacent intergenic region. A similar strategy was used to replace *cdsA* in strain 351 with $cdsA_{D222N}$ from strain 351-D10. In brief, a 500-bp segment from *uppS* (located upstream of *cdsA* in strain 351) was amplified by using primers uppS-F and uppS-R and then digested with XhoI and ClaI. A 504-bp segment encompassing the 5′ end of *rseP* (located downstream of *cdsA*) and the intergenic region between *cdsA* and *rseP* was amplified with primers rseP-F and rseP-R and then digested with EcoRI and NotI (Fig. 1C). These upstream and downstream fragments were cloned sequentially into the corresponding sites of pC326. Plasmid pCdsA-KO was introduced into *S. mitis/oralis* 351 by transformation. *S. mitis/oralis* 351 cultures grown overnight were diluted 100-fold in fresh THB supplemented with 20% heat-inactivated horse serum and 1 mg/ml of the plasmid. Transformation mixtures were incubated for 4 h at 37°C and then plated onto blood agar containing 5 μg/ml of chloramphenicol. Genomic DNA was isolated from chloramphenicol-resistant clones, and the replacement of *cdsA* with *cat* was confirmed by PCR amplification and sequencing. The replacement of *cdsA* in strain 351 with $cdsA_{D222N}$ from 351-D10 was performed by amplifying the upstream 3′ half of $cdsA_{D222N}$ (encompassing the D222N mutation) in *S. mitis/oralis* 351-D10 by using primers *cdsA*-F and *cdsA*-R (Table S1). The resulting fragment, together with the above-mentioned 504-bp fragment, was cloned into pC326. The resulting plasmid ($pCdsA_{D222N}cat$) was introduced into *S. mitis/oralis* 351 by natural transformation and plated onto blood agar containing chloramphenicol and DAP. Genomic DNA was isolated from resistant clones. Subsequently, PCR amplification and DNA sequencing were used to confirm that the nucleotide change (leading to the D222N substitution) had occurred in *cdsA*.

Accession number(s). The genome of *S. mitis/oralis* 351 has been deposited in the NCBI database (BioProject accession number PRJNA358614).

SUPPLEMENTAL MATERIAL

Supplemental material for this article may be found at https://doi.org/10.1128/AAC.02435-16.

TEXT S1, PDF file, 0.2 MB.

ACKNOWLEDGMENTS

NIH grant support includes grants K24-AI114818, R01-AI093749, R21-AI114961, and R21/R33 AI121519 to C.A.A.; R01-AI41513, R01-AI106987, and R21-DE025826 to P.M.S.; K08-AI113317 to T.T.T.; R01-AI039108 to A.S.B.; and R21-AI109266 and R01-AI12400 to M.J.R. C.A.A. and P.M.S. are supported by UT system STARS and VA Merit (1I01BX001653) awards, respectively. J.M.M. is supported by grants INT15/00168 and FIS#02/032 (Instituto de Salud Carlos III, Ministerios de Economía y Competitividad and Sanidad y Consumo, respectively, Madrid, Spain). Part of this work was supported by Merck.

We are indebted to the endocarditis team of the Hospital Clinic of Barcelona. We are grateful to Barbara A. Bensing for technical assistance in *S. mitis/oralis* mutant construction and Danya Alvarez for technical assistance in lipid extraction and analysis. We thank Luke Tallon at the University of Maryland Institute for Genome Sciences for his help with genome sequencing.

J.M.M. has received consulting honoraria and/or research grants from AbbVie, BMS, Cubist, Merck, Novartis, Gilead Sciences, Pfizer, Roche, and ViiV Healthcare. A.S.B. has received research grants from Trellis, ContraFect Corp., and Theravance. C.A.A. has received research funding from Merck, Theravance, Allergan, and The Medicines Company; he is on the speaker bureaus of Pfizer, Merck, Allergan, and The Medicines Company and has served as a consultant for Theravance, The Medicines Company, Merck, Bayer Global, and Allergan. M.J.R. has received research grants and consulting and/or speaking honoraria from Allergan, Cempra, Merck, The Medicines Company, and Theravance. N.N.M. has received a research grant from Cubist Pharmaceuticals.

ADDENDUM IN PROOF

Strain *S. mitis* 351 was identified as an *S. mitis* strain based on standard biotyping and 16S rRNA sequencing. Shortly after this paper was accepted for publication, however, we discovered that this strain is more likely to be a member of the closely related species *S. oralis*, based on average nucleotide identity analysis of the whole genome sequence. The strain has therefore been renamed *S. mitis/oralis* 351 and is so listed in GenBank.

REFERENCES

1. Shelburne SA, Sahasrabhojane P, Saldana M, Yao H, Su X, Horstmann N, Thompson E, Flores AR. 2014. *Streptococcus mitis* strains causing severe clinical disease in cancer patients. Emerg Infect Dis 20:762–771. https://doi.org/10.3201/eid2005.130953.
2. Freifeld AG, Razonable RR. 2014. Viridans group streptococci in febrile neutropenic cancer patients: what should we fear? Clin Infect Dis 59:231–233. https://doi.org/10.1093/cid/ciu264.
3. Prabhu RM, Piper KE, Baddour LM, Steckelberg JM, Wilson WR, Patel R. 2004. Antimicrobial susceptibility patterns among viridans group streptococcal isolates from infective endocarditis patients from 1971 to 1986 and 1994 to 2002. Antimicrob Agents Chemother 48:4463–4465. https://doi.org/10.1128/AAC.48.11.4463-4465.2004.
4. Doern GV, Ferraro MJ, Brueggemann AB, Ruoff KL. 1996. Emergence of high rates of antimicrobial resistance among viridans group streptococci in the United States. Antimicrob Agents Chemother 40:891–894.
5. Sabella C, Murphy D, Drummond-Webb J. 2001. Endocarditis due to *Streptococcus mitis* with high-level resistance to penicillin and ceftriaxone. JAMA 285:2195. https://doi.org/10.1001/jama.285.17.2195.
6. Quinn JP, DiVincenzo CA, Lucks DA, Luskin RL, Shatzer KL, Lerner SA. 1988. Serious infections due to penicillin-resistant strains of viridans streptococci with altered penicillin-binding proteins. J Infect Dis 157:764–769. https://doi.org/10.1093/infdis/157.4.764.
7. Safdar A, Rolston KV. 2006. Vancomycin tolerance, a potential mechanism for refractory gram-positive bacteremia observational study in patients with cancer. Cancer 106:1815–1820. https://doi.org/10.1002/cncr.21801.
8. Garcia-de-la-Maria C, Pericas JM, Del Rio A, Castaneda X, Vila-Farres X, Armero Y, Espinal PA, Cervera C, Soy D, Falces C, Ninot S, Almela M, Mestres CA, Gatell JM, Vila J, Moreno A, Marco F, Miro JM, Hospital Clinic Experimental Endocarditis Study Group. 2013. Early *in vitro* and *in vivo* development of high-level daptomycin resistance is common in mitis group streptococci after exposure to daptomycin. Antimicrob Agents Chemother 57:2319–2325. https://doi.org/10.1128/AAC.01921-12.
9. Akins RL, Katz BD, Monahan C, Alexander D. 2015. Characterization of high-level daptomycin resistance in viridans group streptococci developed upon in vitro exposure to daptomycin. Antimicrob Agents Chemother 59:2102–2112. https://doi.org/10.1128/AAC.04219-14.
10. Pogliano J, Pogliano N, Silverman JA. 2012. Daptomycin-mediated reorganization of membrane architecture causes mislocalization of essential cell division proteins. J Bacteriol 194:4494–4504. https://doi.org/10.1128/JB.00011-12.
11. Arias CA, Panesso D, McGrath DM, Qin X, Mojica MF, Miller C, Diaz L, Tran TT, Rincon S, Barbu EM, Reyes J, Roh JH, Lobos E, Sodergren E, Pasqualini R, Arap W, Quinn JP, Shamoo Y, Murray BE, Weinstock GM. 2011. Genetic basis for in vivo daptomycin resistance in enterococci. N Engl J Med 365:892–900. https://doi.org/10.1056/NEJMoa1011138.
12. Muller A, Wenzel M, Strahl H, Grein F, Saaki TN, Kohl B, Siersma T, Bandow JE, Sahl HG, Schneider T, Hamoen LW. 24 October 2016. Daptomycin inhibits cell envelope synthesis by interfering with fluid membrane microdomains. Proc Natl Acad Sci U S A https://doi.org/10.1073/pnas.1611173113.
13. Tran TT, Munita JM, Arias CA. 2015. Mechanisms of drug resistance: daptomycin resistance. Ann N Y Acad Sci 1354:32–53. https://doi.org/10.1111/nyas.12948.
14. Taylor SD, Palmer M. 28 May 2016. The action mechanism of daptomycin. Bioorg Med Chem https://doi.org/10.1016/j.bmc.2016.05.052.
15. Zhang T, Muraih JK, Tishbi N, Herskowitz J, Victor RL, Silverman J, Uwumarenogie S, Taylor SD, Palmer M, Mintzer E. 2014. Cardiolipin prevents membrane translocation and permeabilization by daptomycin. J Biol Chem 289:11584–11591. https://doi.org/10.1074/jbc.M114.554444.
16. Tran TT, Panesso D, Mishra NN, Mileykovskaya E, Guan Z, Munita JM, Reyes J, Diaz L, Weinstock GM, Murray BE, Shamoo Y, Dowhan W, Bayer AS, Arias CA. 2013. Daptomycin-resistant *Enterococcus faecalis* diverts the antibiotic molecule from the division septum and remodels cell membrane phospholipids. mBio 4:e0028111584–13. https://doi.org/10.1128/mBio.00281-13.
17. Liu X, Yin Y, Wu J, Liu Z. 2014. Structure and mechanism of an intramembrane liponucleotide synthetase central for phospholipid biosynthesis. Nat Commun 5:4244. https://doi.org/10.1038/ncomms5244.
18. Baba T, Ara T, Hasegawa M, Takai Y, Okumura Y, Baba M, Datsenko KA, Tomita M, Wanner BL, Mori H. 2006. Construction of *Escherichia coli* K-12 in-frame, single-gene knockout mutants: the Keio collection. Mol Syst Biol 2:2006.0008.
19. Ganong BR, Raetz CR. 1982. Massive accumulation of phosphatidic acid in conditionally lethal CDP-diglyceride synthetase mutants and cytidine auxotrophs of *Escherichia coli*. J Biol Chem 257:389–394.
20. Oliver PM, Crooks JA, Leidl M, Yoon EJ, Saghatelian A, Weibel DB. 2014. Localization of anionic phospholipids in *Escherichia coli* cells. J Bacteriol 196:3386–3398. https://doi.org/10.1128/JB.01877-14.
21. Mishra NN, Liu GY, Yeaman MR, Nast CC, Proctor RA, McKinnell J, Bayer AS. 2011. Carotenoid-related alteration of cell membrane fluidity impacts *Staphylococcus aureus* susceptibility to host defense peptides.

Antimicrob Agents Chemother 55:526–531. https://doi.org/10.1128/AAC.00680-10.
22. Mishra NN, Yang SJ, Sawa A, Rubio A, Nast CC, Yeaman MR, Bayer AS. 2009. Analysis of cell membrane characteristics of *in vitro*-selected daptomycin-resistant strains of methicillin-resistant *Staphylococcus aureus*. Antimicrob Agents Chemother 53:2312–2318. https://doi.org/10.1128/AAC.01682-08.
23. Mishra NN, McKinnell J, Yeaman MR, Rubio A, Nast CC, Chen L, Kreiswirth BN, Bayer AS. 2011. *In vitro* cross-resistance to daptomycin and host defense cationic antimicrobial peptides in clinical methicillin-resistant *Staphylococcus aureus* isolates. Antimicrob Agents Chemother 55:4012–4018. https://doi.org/10.1128/AAC.00223-11.
24. Lopez-Amoros R, Castel S, Comas-Riu J, Vives-Rego J. 1997. Assessment of *E. coli* and *Salmonella* viability and starvation by confocal laser microscopy and flow cytometry using rhodamine 123, DiBAC4(3), propidium iodide, and CTC. Cytometry 29:298–305. https://doi.org/10.1002/(SICI)1097-0320(19971201)29:4<298::AID-CYTO6>3.0.CO;2-6.
25. Reyes J, Panesso D, Tran TT, Mishra NN, Cruz MR, Munita JM, Singh KV, Yeaman MR, Murray BE, Shamoo Y, Garsin D, Bayer AS, Arias CA. 2015. A *liaR* deletion restores susceptibility to daptomycin and antimicrobial peptides in multidrug-resistant *Enterococcus faecalis*. J Infect Dis 211:1317–1325. https://doi.org/10.1093/infdis/jiu602.
26. Mishra NN, Bayer AS, Tran TT, Shamoo Y, Mileykovskaya E, Dowhan W, Guan Z, Arias CA. 2012. Daptomycin resistance in enterococci is associated with distinct alterations of cell membrane phospholipid content. PLoS One 7:e43958. https://doi.org/10.1371/journal.pone.0043958.
27. Peleg AY, Miyakis S, Ward DV, Earl AM, Rubio A, Cameron DR, Pillai S, Moellering RC, Jr, Eliopoulos GM. 2012. Whole genome characterization of the mechanisms of daptomycin resistance in clinical and laboratory derived isolates of *Staphylococcus aureus*. PLoS One 7:e28316. https://doi.org/10.1371/journal.pone.0028316.
28. Hachmann AB, Angert ER, Helmann JD. 2009. Genetic analysis of factors affecting susceptibility of *Bacillus subtilis* to daptomycin. Antimicrob Agents Chemother 53:1598–1609. https://doi.org/10.1128/AAC.01329-08.
29. Garcia-de-la-Maria CPJ, Armero Y, Moreno A, Mishra NN, Rybak MJ, Tran TT, Arias CA, Sullam PM, Xiong YQ, Bayer AS, Miro JM. 2016. High-level daptomycin-resistant (Dap-R) *Streptococcus mitis* is virulent in experimental endocarditis (Ee) and enhances survivability during Dap treatment vs. its Dap-susceptible (Dap-S) parental strain, abstr SUNDAY-335. Abstr ASM Microbe 2016.
30. Kikuchi S, Shibuya I, Matsumoto K. 2000. Viability of an *Escherichia coli pgsA* null mutant lacking detectable phosphatidylglycerol and cardiolipin. J Bacteriol 182:371–376. https://doi.org/10.1128/JB.182.2.371-376.2000.
31. Sutterlin HA, Zhang S, Silhavy TJ. 2014. Accumulation of phosphatidic acid increases vancomycin resistance in *Escherichia coli*. J Bacteriol 196:3214–3220. https://doi.org/10.1128/JB.01876-14.
32. Bayles KW. 2007. The biological role of death and lysis in biofilm development. Nat Rev Microbiol 5:721–726. https://doi.org/10.1038/nrmicro1743.
33. Claverys JP, Havarstein LS. 2007. Cannibalism and fratricide: mechanisms and raisons d'etre. Nat Rev Microbiol 5:219–229. https://doi.org/10.1038/nrmicro1613.
34. Diaz L, Tran TT, Munita JM, Miller WR, Rincon S, Carvajal LP, Wollam A, Reyes J, Panesso D, Rojas NL, Shamoo Y, Murray BE, Weinstock GM, Arias CA. 2014. Whole-genome analyses of *Enterococcus faecium* isolates with diverse daptomycin MICs. Antimicrob Agents Chemother 58:4527–4534. https://doi.org/10.1128/AAC.02686-14.
35. Mileykovskaya E, Dowhan W. 2000. Visualization of phospholipid domains in *Escherichia coli* by using the cardiolipin-specific fluorescent dye 10-*N*-nonyl acridine orange. J Bacteriol 182:1172–1175. https://doi.org/10.1128/JB.182.4.1172-1175.2000.
36. Mishra NN, Bayer AS, Weidenmaier C, Grau T, Wanner S, Stefani S, Cafiso V, Bertuccio T, Yeaman MR, Nast CC, Yang SJ. 2014. Phenotypic and genotypic characterization of daptomycin-resistant methicillin-resistant *Staphylococcus aureus* strains: relative roles of *mprF* and *dlt* operons. PLoS One 9:e107426. https://doi.org/10.1371/journal.pone.0107426.
37. Tsai M, Ohniwa RL, Kato Y, Takeshita SL, Ohta T, Saito S, Hayashi H, Morikawa K. 2011. *Staphylococcus aureus* requires cardiolipin for survival under conditions of high salinity. BMC Microbiol 11:13. https://doi.org/10.1186/1471-2180-11-13.
38. Bayer AS, Prasad R, Chandra J, Koul A, Smriti M, Varma A, Skurray RA, Firth N, Brown MH, Koo SP, Yeaman MR. 2000. In vitro resistance of *Staphylococcus aureus* to thrombin-induced platelet microbicidal protein is associated with alterations in cytoplasmic membrane fluidity. Infect Immun 68:3548–3553. https://doi.org/10.1128/IAI.68.6.3548-3553.2000.
39. Galens K, Orvis J, Daugherty S, Creasy HH, Angiuoli S, White O, Wortman J, Mahurkar A, Giglio MG. 2011. The IGS standard operating procedure for automated prokaryotic annotation. Stand Genomic Sci 4:244–251. https://doi.org/10.4056/sigs.1223234.
40. Cingolani P, Platts A, Wang LL, Coon M, Nguyen T, Wang L, Land SJ, Lu X, Ruden DM. 2012. A program for annotating and predicting the effects of single nucleotide polymorphisms, SnpEff: SNPs in the genome of *Drosophila melanogaster* strain w1118;iso-2;iso-3. Fly (Austin) 6:80–92. https://doi.org/10.4161/fly.19695.
41. Mitchell J, Siboo IR, Takamatsu D, Chambers HF, Sullam PM. 2007. Mechanism of cell surface expression of the *Streptococcus mitis* platelet binding proteins PblA and PblB. Mol Microbiol 64:844–857. https://doi.org/10.1111/j.1365-2958.2007.05703.x.
42. Seo HS, Xiong YQ, Mitchell J, Seepersaud R, Bayer AS, Sullam PM. 2010. Bacteriophage lysin mediates the binding of *Streptococcus mitis* to human platelets through interaction with fibrinogen. PLoS Pathog 6:e1001047. https://doi.org/10.1371/journal.ppat.1001047.